Proceedings of the 17th World Congress
The International Federation of Automatic Control
Seoul, Korea, July 6-11, 2008

Impedance Compensation of Flexible Joint Actuator for Ideal Force Mode Control

Kyoungchul Kong. Joonbum Bae
Masayoshi Tomizuka

Mechanical Engineering Department, University of California, Berkeley, CA 94720, USA
(e-mail:{kckong, jbbae, tomizuka}@ me.berkeley.edu)

Abstract: To realize an ideal force control of robots interacting with humans, a very precise actuation system with zero impedance is desired. A flexible joint actuator may serve for this purpose. This paper presents the design of control algorithms to compensate for the impedance in the flexible joint actuator. To generate the torque as desired, a spring is installed between a motor and a human joint, and the motor is controlled to produce the proper spring deflection. When the desired torque is zero, the motor must follow human joint motion, which requires that the friction and inertia of the motor are compensated. Mechanical properties of a human body are not fixed, while they represent the load to the flexible joint actuator. The disturbance observer method is applied to make the flexible joint actuator precisely generate the desired torque under such time-varying conditions. Based on the nominal model preserved by the disturbance observer, feedback and feedforward controllers are optimally designed for the desired performance: i.e. the flexible joint actuator 1) exhibits very low impedance and 2) generates the desired torque precisely during interacting with a human. The effectiveness of the proposed design is verified by experiments.

1. INTRODUCTION

Mechatronic applications to better quality of life are gaining increasing attention. Active assistive devices such as motorized wheel chairs and active prosthetics are representative cases. They have improved the mobility of many people with disabilities and helped them engage in daily activities as normal people. Recently, power assistive devices based on robotics technologies are being developed in the form of wearable robots, the purpose of which is to aid physically impaired people.

It is desired that the controllers for human-robot interaction, such as the assistive controller and the impedance controller, may assume that the actuators are operated in an ideal force (or torque) control mode (Hogan, 1985)(Riener *et al.,* 2005). The ideal force mode implies: 1) the actuator has zero impedance so that it is perfectly back-drivable, and 2) the force (torque) output is exactly proportional to the control input. Researchers have tried to find such actuators for the ideal human-robot inter-action. In spite of such efforts, the lack of a suitable actuator is still evident. Recently, progresses have been made to overcome nonideal problems of actuators by applying an algorithmic compensator. For example, Buerger and Hogan introduced the complimentary stability and loop shaping method to design the compensator computationally (Buerger and Hogan, 2007). From the viewpoint of both hardware and controller designs, the flexible joint actuator is noteworthy (Kong and Tomizuka, 2007). In this case, a spring is installed between the actuator and human joint, and plays the role of an energy buffer as well as a force sensor. The force is generated from the differential position or deflection of the spring, which is controlled by a position controller. In this case, compensation of the impedance is accomplished based on a position control method. The spring isolates the human joint from undesired factors of the motor including rotor inertia and nonlinearities, but it also gives challenges in the design of a controller. Interacting with human, the motor dynamics as seen by the controller is time varying. Therefore, for the desired performance, it requires a well-designed feedback controller which robustly rejects the undesired factors under time-varying conditions. Namely, the controller of the flexible joint actuator should meet the following performance objectives:

1) it rejects every undesired factor in the motor so that the actuator precisely generates the torque as desired

2) it makes the overall flexible joint actuator have zero impedance so that it does not disturb human

3) it guarantees the robust performance of the actuator in the environment interacting with human.

In this paper, the design of controllers for the flexible joint actuator is discussed. To assure the robust performance of the flexible joint actuator, a disturbance observer is used as well as the feedback and feedforward controllers.

2. CONTROLLER DESIGN FOR FLEXIBLE JOINT ACTUATOR

2.1 System Modeling

Figure 1 shows the flexible joint actuator. Two encoders ((a) and (f) in the figure) are installed to measure the spring deflection as well as the motor angle. Potentiometers ((e) and (g)) are for initialization of the incremental encoders. The frame ((c) in the figure) is attached to a human joint such that the joint is assisted.

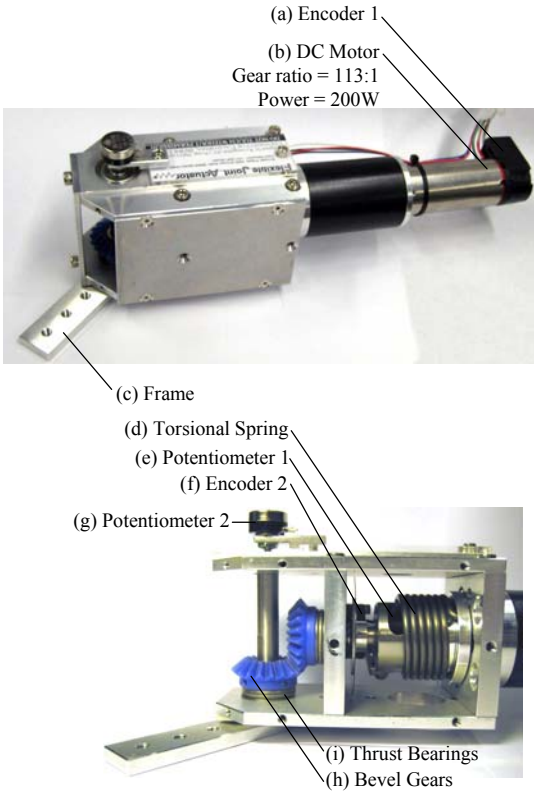

Fig. 1 Mechanical design of the flexible joint actuator

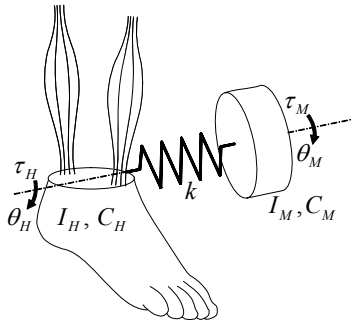

Fig. 2 Schematic plot of human joint and flexible joint actuator

The flexible joint actuator installed on a human joint is depicted in Fig. 2, where I_H and C_H are the inertia and damping coefficient of human joint, and I_M and C_M are those of the geared motor, respectively. The motor and the human joint are connected via a spring with spring constant k. τ_M and τ_H represent the human muscular torque and the motor torque, and θ_M and θ_H are the angles of the human joint and the motor respectively. The flexible joint actuator is a multi-input and multi-output system where inputs are the actuator torque and the human muscular torque, and outputs are the actuator angle and the human joint angle. The controlled output is the spring torque which is proportional to the spring deflection, i.e. the difference between the actuator and the human joint angle.

The governing equation for the system in Fig. 2 is

$$\begin{bmatrix} I_M & 0 \\ 0 & I_H \end{bmatrix}\ddot{\Theta} + \begin{bmatrix} C_M & 0 \\ 0 & C_H \end{bmatrix}\dot{\Theta} + \begin{bmatrix} k & -k \\ -k & k \end{bmatrix}\Theta = \begin{bmatrix} \tau_M \\ \tau_H - mgl\sin(\theta_H) \end{bmatrix} \quad (1)$$

where, Θ is $[\theta_M \ \theta_H]^T$, m is the mass of human body segment, g is the gravity constant, and l is the distance between a joint and the center of mass of the body segment. The dynamic equation assumes that there is no constraint imposed on either the motor or the human joint. The joint, however, is subject to constraints during some motion phases. For example, if the foot is touching the ground, it may be reasonable to assume that the human side of the spring is grounded as shown in Fig. 3(b). In this case, (1) no longer applies. Thus the human joint actuation system requires multiple dynamic models for complete description of its dynamic behavior. A possible approach to handle such a system is the discrete event system approach. In this paper, we explore an approach to design a controller for a nominal model. Actual dynamics is regarded as perturbed dynamics.

Assume that there is a relation between the motor angle and the spring deflection such that

$$\frac{E(s)}{\theta_M(s)} = \alpha(s) \quad (2)$$

where $E(s) = [\theta_M(s) - \theta_H(s)]$. $\alpha(s)$ is obtained by setting $\tau_H = 0$ in (1) which assumes that the muscular power of human is negligible, i.e.

$$\alpha(s) = \frac{I_H s^2 + C_H s + mgl}{I_H s^2 + C_H s + k + mgl} \quad (3)$$

where $\sin(\theta)$ has been approximated by θ. The approximation in (3) is meaningful when actuator power is greater than human power, or the human is a physically impaired person. The magnitude of $\alpha(s)$ depends on the physical properties of the human body segment. Namely, $\alpha(s)$ is a transfer function resulted from human-robot interaction which is unknown and time-varying. By Hooke's law, the relation between the motor angle and the spring torque is obtained as

$$\tau_A(s) = kE(s) = k\alpha(s)\theta_M(s) \quad (4)$$

By Newton's third law, the spring torque is exerted to the motor system as well as the human body. Therefore the dynamics of the motor part is

$$I_M\ddot{\theta}_M + C_M\dot{\theta}_M = \tau_M(t) - \tau_A(t) \quad (5)$$

Combining (4) and (5), a transfer function from τ_M to θ_M is obtained as

$$P(s) = \frac{1}{I_M s^2 + C_M s + \alpha(s)k} \in \Psi(s) \quad (6)$$

where $\Psi(s)$ represents a possible model set of the flexible joint actuator. Note that the model is time-varying as $\alpha(s)$ changes due to human-robot interaction. Fig. 3 shows two extreme cases.

Case 1

Case 1 in Fig. 3 applies during swinging of a leg. During the swing motion in a normal gait, movements of ankle and knee joints are large. In this case, it is a reasonable assumption that the joint motion is mainly resulted by the gravity and the assistive torque. The transfer function from $\tau_M(s)$ to $\theta_M(s)$ is

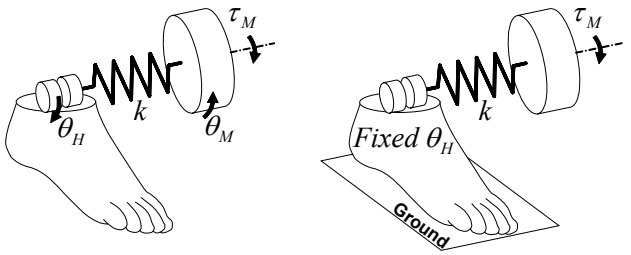

(a) Case 1 (b) Case 2

Fig. 3 Two possible cases of human joint

$$P_1(s) = \frac{1}{I_M s^2 + C_M s + \alpha(s)k} \in \Psi(s) \tag{7}$$

where $\alpha(s)$ is given by (3) and its magnitude depends on the physical properties of human body segments.

Case 2

During the stance motion in a normal gait and standing up motion, movements of ankle and knee joints are slow while the required joint torques are large. Therefore, the motion of the actuator is much larger than that of the human joint. Moreover, since the body segment is grounded, a constraint is imposed on the human joint. This may be regarded as a significant increase of I_H in (3), i.e. $I_H >> 1$, which results in $\alpha(s) \approx 1$, i.e.

$$P_2(s) = \frac{1}{I_M s^2 + C_M s + k} \in \Psi(s) \tag{8}$$

Since $P_2(s)$ in (8) has the minimum order in the possible model set and does not require properties of human body which are usually difficult to measure, the transfer function of (8) is used as a nominal model in this paper, i.e. $P_n(s) = P_2(s)$.

2.2 Optimal PD Control

To improve the tracking performance, a feedback control algorithm is required. For the design of the controller, the control loop is reconfigured as shown in Fig. 4. The aim of the controller ($C(s)$ in the figure) is to maintain the desired spring deflection regardless of variations of the system model.

Fig. 5 shows the location of poles and zeros of the open loop transfer function from τ_M to E in Fig. 4. By increasing I_H in $\alpha(s)$, poles and zeros converge to the points labeled (d) in Fig. 5. Note that there is a weakly damped complex pole-zero pair and the pair moves towards the imaginary axis as I_H is increased. As I_H approaches infinity, they asymptotically cancel each other, and the open loop transfer function is asymptotic to (8).

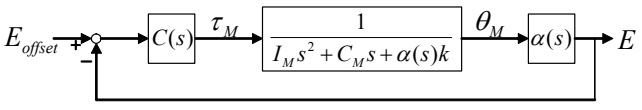

Fig. 4 Block diagram of the Joint Controller: E_{offset} is the desired spring deflection.

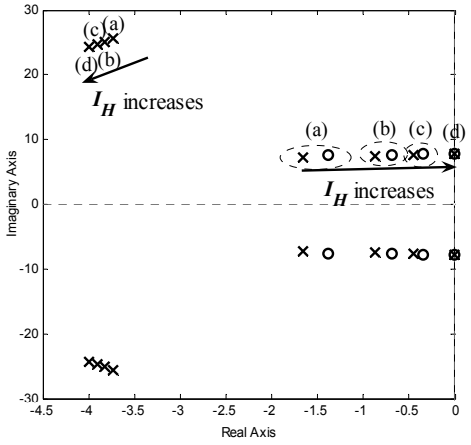

Fig. 5 Poles and zeros of the open loop transfer function: (a), (b), (c) and (d) apply for the ankle joint of the 50%^{ile} female, the knee joint of the 50%^{ile} female, the knee joint of the 50%^{ile} male and the constrained joint respectively (Winter, 1990).

A simple and effective controller is a PD (Proportional-Derivative) controller. A quantitative way to tune the PD control gains is to apply the LQ (Linear Quadratic) method. The LQ method is applicable when the nominal model in (8) is expressed in the state space. Moreover, if the state consists of position and velocity in the second order model, the LQ method provides the optimal PD gains. In the case of $P_2(s)$ in (8), the state space model is expressed as

$$\begin{bmatrix} \ddot{\theta} \\ \dot{\theta} \\ \theta_M \end{bmatrix} = \left[\begin{array}{cc|c} -C_M/I_M & -k/I_M & 1/I_M \\ \hline 1 & 0 & 0 \\ 0 & 1 & 0 \end{array}\right] \begin{bmatrix} \dot{\theta} \\ \theta \\ \tau_M \end{bmatrix} \tag{9}$$

where $\dot{\theta}$ and θ define the state, τ_M is the input and θ_M is the output.

The LQ performance index is

$$\begin{aligned} J &= \int_0^\infty [\theta_M^2(t) + R\tau_M^2(t)]dt \\ &= \int_0^\infty \left[\begin{bmatrix} \dot{\theta} \\ \theta \end{bmatrix}^T C^T C \begin{bmatrix} \dot{\theta} \\ \theta \end{bmatrix} + R\tau_M^2(t) \right] dt \end{aligned} \tag{10}$$

Solving the Riccati equation based on the state space model in (9), the control gains are obtained as follows

$$0 = A^T P + PA - PBR^{-1}B^T P + C^T C \tag{11}$$

$$K = R^{-1}B^T P \tag{12}$$

where K is $[K_D\ K_P]^T$. P is the positive definite solution of the Riccati equation in (11) where R is a penalizing factor of control input. A, B and C are as defined in (9). Since R is scalar, we have only one degree of freedom for designing the feedback controller. R should be sufficiently small so that the control system has an adequate bandwidth.

2.3 Robustness Enhancement

Normally, the control performance in terms of output tracking becomes better if the PD control gains are increased. However, since the PD control gains may be increased only

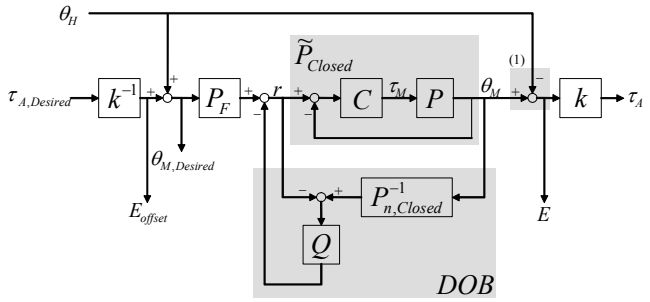

Fig. 6 Block diagram of the overall joint control system: The overall control method is to compensate for impedance in the flexible joint actuator.

in a limited range due to practical problems such as noise and instability caused by discretization, a better robust control method may be required to achieve the desired performance objectives. It is desirable to make the magnitude of the closed loop frequency response close to one over a sufficiently large frequency range. The bandwidth of the human joint is about 8Hz (Winter, 1990) and the frequency response should be flat at least over this frequency range. Note that the closed loop transfer function strongly depends on $\alpha(s)$, which makes the dynamic transient vary significantly. In order to overcome this problem, the DOB (Disturbance Observer) may be introduced as shown in Fig. 6.

In general, the DOB may be used to:

1) estimate and cancel disturbance, and

2) compensate for the variation of plant dynamics by treating the variation as an equivalent disturbance.

In this application, the DOB is used more for the second objective although the disturbance cancellation is taking place also. For the basic properties of DOB, see (Lee and Tomizuka, 1996).

It should be noted that the DOB is applied for the motor part only, i.e. the human joint angle is not fed into the DOB in Fig. 6. Since the DOB is capable of rejecting exogenous disturbances, it increases the motor impedance significantly. Moreover, if E is fed back into the DOB, the human joint angle θ_H may be regarded as a disturbance (see (1) in Fig. 5) and rejected, or resisted, by the DOB. Since this is undesirable for human-robot interaction, the human joint angle should not be fed into the DOB.

The overall control scheme in Fig. 6 is as follows:

1) First, the desired spring deflection E_{offset} is obtained from the desired torque on-line. Adding the human joint angle θ_H, the desired position of the motor $\theta_{M,Desired}$ is obtained. Note that if the desired torque is zero, then $\theta_{M,Desired}$ is the same as θ_H.

2) Second, the feedforward filter (P_F in Fig. 6) is applied for compensating the dynamics of motor part. P_F is designed based on the nominal closed loop model. In fact, the tracking performance of the motor is significantly improved by this feedforward filter.

3) Third, the PD controller (C in Fig. 6) is applied to attenuate the model variation. It allows increasing the bandwidth of DOB so that the performance of the overall system is improved significantly. The PD control gains are optimally obtained from (11) and (12) based on the nominal model in (8).

4) Finally, the DOB compensates for model variations due to human-robot interaction, and rejects exogenous disturbance. It makes the motor part behave as the nominal model. Therefore, the feedforward filter P_F can show the optimal performance.

It is assumed that the closed loop transfer function $\tilde{P}_{Closed}(s)$ in Fig. 6 is expressed as

$$\tilde{P}_{Closed}(s) = P_{n,Closed}(s)\left[1 + \Delta_{Closed}(s)\right] \tag{13}$$

where $P_{n,Closed}(s)$ is the nominal closed loop dynamics obtained from $P_n(s)$ in (8) under PD control, i.e.

$$P_{n,Closed}(s) = \frac{P_n(s)C(s)}{1 + P_n(s)C(s)} \tag{14}$$

and $\Delta_{Closed}(s)$ is

$$\Delta_{Closed}(s) = \frac{(1-\alpha(s))k}{I_M s^2 + C_M s + \alpha(s)k + C(s)} \tag{15}$$

Note that the closed loop transfer function in (14) is used as a nominal model in the design of DOB.

In the design of DOB, it is important to select the filter labeled Q in Fig. 6. The order of $Q(s)$ must be selected so that $Q(s)P^{-1}_{2,Closed}(s)$ is realizable. The remaining two conditions ((16) and (17)) make the closed loop system with DOB robust in terms of performance and stability. Namely, the DOB is effective where

$$|Q(j\omega)| = 1 \ for \ some \ \omega \in \Re \tag{16}$$

The stability condition introduces another constraint:

$$\left\| Q(j\omega)\Delta_{Closed}(j\omega) \right\|_\infty < 1 \tag{17}$$

Equations (16) and (17) require that the magnitude of the model uncertainty should be less than one over a sufficiently large frequency range. Since the magnitude of the model uncertainty in (15) decreases as the PD control gains increase, the Q filter can be designed to have a sufficiently large bandwidth.

The feedforward filter P_F applies the pole-zero cancellation method such that

$$P_F(s) = P_{n,Closed}^{-1}(s)P_R(s) \tag{18}$$

where $P_{n,Closed}(s)$ is as defined in (14). Since the inverse of the transfer function is usually unrealizable, $P_R(s)$ has been introduced for realizability of the feedforward filter. Note that the magnitude of $P_R(j\omega)$ should be close to one over a sufficiently large frequency range, and its bandwidth should be the same or larger than that of the Q filter.

Arranging (10), (14) and (18) based on the control structure in Fig. 6, we obtain the transfer function of the overall flexible joint actuator as follows

$$\begin{aligned}\tau_A(s) &= k[\theta_M(s) - \theta_H(s)] \\ &= Z_\tau(s)\tau_{A,Desired}(s) + Z_H(s)\theta_H(s) + Z_d(s)d(s)\end{aligned} \tag{19}$$

where

$$Z_\tau(s) = \frac{P_R(s)a(s)}{a(s)Q(s) + b(s)[1-Q(s)]} \tag{20}$$

$$Z_H(s) = k\left[Z_\tau(s) - 1\right] \tag{21}$$

$$Z_d(s) = k\frac{[1-Q(s)]}{a(s)Q(s) + b(s)[1-Q(s)]}\frac{P(s)}{1 + P_n(s)C(s)} \tag{22}$$

$$a(s) = \frac{P(s)}{P_n(s)}, \quad b(s) = \frac{1 + P(s)C(s)}{1 + P_n(s)C(s)} \tag{23}$$

$Z_H(s)$, $Z_\tau(s)$ and $Z_d(s)$ represent the transfer functions to the torque output from the human joint angle $\theta_H(s)$, the desired output $\tau_{A,Desired}(s)$ and the exogenous disturbance input $d(s)$, respectively. The performance objectives are:

$$Z_H(j\omega) = 0 \quad \forall\omega \in [0 \;\; 16\pi) \tag{24}$$

$$Z_\tau(j\omega) = 1 \quad \forall\omega \in [0 \;\; 16\pi) \tag{25}$$

$$Z_d(j\omega) = 0 \quad \forall\omega \in [0 \;\; 16\pi) \tag{26}$$

where 8Hz represents the frequency range of human motion. (24) implies that the flexible joint actuator does not generate the resistive torque to the human joint motion, i.e. motor impedance is decreased. (25) represents that the actuator generates the torque as desired precisely. Finally, (26) means that the exogenous disturbance does not affect the torque output.

Note that the performance objectives are satisfied if Q and P_R are designed such that

$$Q(j\omega) = 1 \; and \; P(j\omega) = 1 \quad \forall\omega \in [0 \;\; 16\pi) \tag{27}$$

3. PERFORMANCE ANALYSIS BY EXPERIMENTS

Once the flexible joint actuator is stabilized by designing the overall control system in Fig. 6, it is desired to verify the following performance objectives:

1) Capability of generating the desired torque precisely,

2) Capability of generating the desired torque with a sufficiently large frequency bandwidth, and

3) Capability of rejecting the undesired disturbances including the rotor inertia and any of nonlinearities, i.e. the flexible joint actuator has zero impedance.

3.1 Motor Impedance Test

A flexible joint actuator in Fig. 1 is used to verify the performance objectives stated above. In experiments, a spring is used as a torque sensor as well as the energy buffer.

As mentioned already, actuators for human-robot interaction should have low mechanical impedance. Otherwise, human has to make an additional effort to overcome the resistive forces. Fig. 7 shows the relation between the actual resistive torques and the angular velocities under the proposed control system when the desired torque output is zero. To exert the precise angular velocity to the flexible joint actuator from the load side, an additional motor that has large impedance was attached at the frame ((c) in Fig. 1). For comparison of the performance, Fig. 7 also shows the results with PD control and open loop control. By applying the proposed control system, the measured torque is closed to zero (see Proposed Control line in Fig. 7), which means no resistive torque is generated regardless of motion of the frame. For more quantitative comparison, the curve fits are obtained (continuous lines in Fig. 7) with the following fitting function,

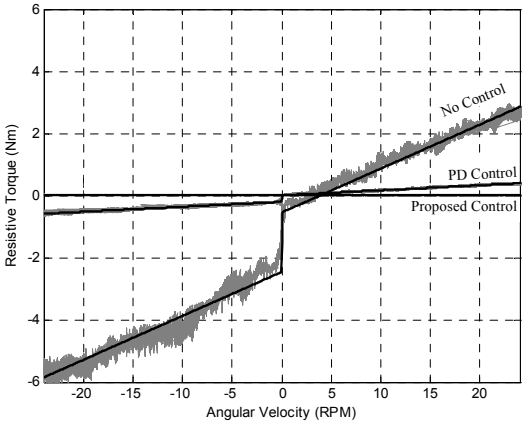

Fig. 7 Motor impedance test about angular velocity: the desired torque output is zero

TABLE I. Coefficients of Motor Impedance

Control Method	a_1 Bias[3]	a_2 Friction[4]	a_3 Linear Damping[5]
No Control	-1.509×10^{0}	9.572×10^{-1}	1.414×10^{-1}
PD Control[1]	-9.534×10^{-2}	1.040×10^{-1}	1.614×10^{-2}
Proposed Control[2]	1.311×10^{-2}	1.464×10^{-3}	-2.941×10^{-4}

Each number shows the coefficient obtained by the curve fit based on (28).
1,2) See block diagrams in Fig. 4 and Fig. 6, respectively.
3,4,5) use the units of [Nm], [Nm] and [Nm/(rad/s)], respectively.

$$f(\omega) = a_1 + a_2\,\mathrm{sgn}(\omega) + a_3\omega \tag{28}$$

where a_1, a_2 and a_3 represent terms due to bias, nonlinear friction and linear damping, respectively. For the desired performance, i.e. to have zero motor impedance, all parameters in (28) should be zero. Table 1 shows the obtained parameters for each control method. Note that the magnitude of each parameter is significantly decreased by the proposed control system.

Fig. 8 shows the relation between the generated torques and the desired torques under the proposed control method when the angular velocity is fixed to zero, i.e. the frame ((c) in Fig. 1) was fixed mechanically. This setup corresponds to Case 2 in Fig. 3. Fig. 8 verifies that the flexible joint actuator controlled by the proposed control system generates torques as desired precisely. Applying the proposed control system, the linearity between desired torque and generated torque is achieved and the bias is removed.

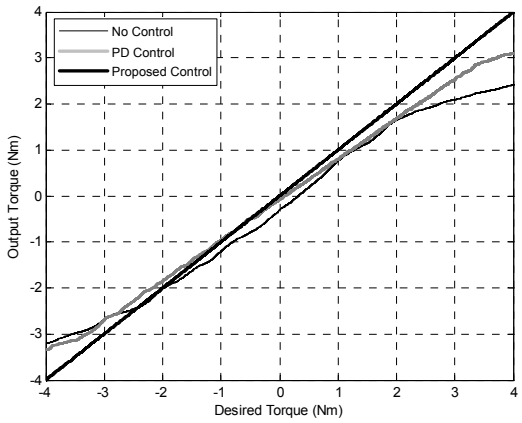

Fig. 8 Linearity test about control input: the angular velocity of rotor is fixed to zero

3.2 Frequency Response Analysis

It is required that the flexible joint actuator generates the desired torque over a sufficiently large frequency range. Fig. 9 shows the frequency responses of the flexible joint actuator controlled by the proposed control system. An experimental setup for frequency response analysis is also the same as in Fig. 1, but a mass was attached to impose the inertia to the flexible joint actuator. Otherwise, the flexible joint actuator easily saturates at the maximum velocity. This setup corresponds to Case 1 in Fig. 3. It is known that the human motion contains frequency components up to 8Hz (Winter, 1990). Note that the flexible joint actuator with the overall control system proposed in this paper generates the desired torque properly up to about 10Hz.

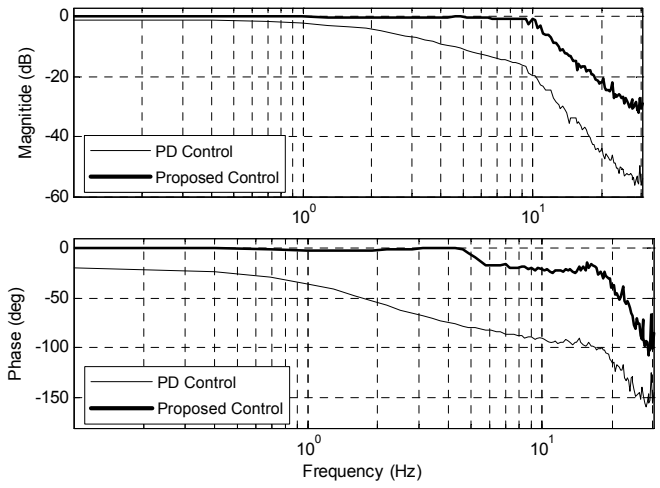

Fig. 9 Frequency response of each control scheme

4. CONCLUSION

In the flexible joint actuator, a spring is installed between a human joint and a motor as an energy buffer. By controlling the motor part with a position control method, the torque is precisely generated via the spring deflection.

The use of spring introduces challenges in the design of controllers. In this paper, the optimal PD control, the feedforward control and the disturbance observer were applied to the design of controllers for the flexible joint actuator. It was shown that the proposed control method meets the desired performances and that the flexible joint actuator generates the torque as desired precisely and its impedance has been decreased significantly. The performance objectives were also verified by experiments.

The flexible joint actuator in this paper may provide a good solution for actuators in human-robot interaction. Since the control method does not require physical properties of the human body, it is not necessary to design the controllers for each individual. It allows precise force (or torque) mode control, and it provides the foundation to the design of higher level controls for human-robot interaction.

REFERENCES

Buerger, S. P. and Hogan, N. (2007). Complementary Stability and Loop Shaping for Improved Human-Robot Interaction. *IEEE Transactions on Robotics*, **Vol. 23**, No. 2, pp. 232-244.

Hogan, N. (1985). Impedance control: An approach to manipulation, parts I, II, III. *Journal of Dynamic Systems, Measurement and Control*, **Vol. 107**, pp. 1-23.

Kong, K. and Tomizuka, M. (2007). Flexible Joint Actuator for Patient's Rehabilitation Device. *Proceeding of the IEEE International Symposium on Robot and Human Interactive Communication (ROMAN).*

Lee, H. and Tomizuka, M. (1996). Robust motion controller design for high-accuracy positioning systems. *IEEE Transactions on Industrial Electronics*, **Vol. 43**, No. 1, pp. 48-55.

Riener, R., Lünenburger, L., Jezernik, S., Anderschitz, M., Colombo, G. and Dietz, V. (2005). Patient-Cooperative Strategies for Robot-Aided Treadmill Training: First Experimental Results. *IEEE Transactions on Neural Systems and Rehabilitation Engineering*, **Vol. 13**, No. 3, pp. 380-394.

Winter, D. (1990), *Biomechanics and Motor Control of Human Movement*, Wiley-Interscience Publication.